IEEE Access
Multidisciplinary | Rapid Review | Open Access Journal

Received September 12, 2020, accepted September 26, 2020, date of publication October 6, 2020, date of current version October 15, 2020.

Digital Object Identifier 10.1109/ACCESS.2020.3029219

A Design of Low Profile Microstrip Patch Antenna With Bandwidth Enhancement

CHAO SUN

Plasma Electromagnetic Physics Laboratory (PEPL), School of Aerospace Science and Technology, Xidian University, Xi'an 710071, China
Key Laboratory of the Ministry of Education of China, School of Aerospace Science and Technology, Xidian University, Xi'an 710071, China

e-mail: sunchao1989913@163.com

This work was supported in part by the National Natural Science Foundation of China under Grant 61627901 and Grant 61801343.

ABSTRACT It is known that for a microstrip antenna (patch antenna) resonant in a single mode, if the height of the antenna is strictly limited, the bandwidth is narrow, and the performance at the side frequencies is worse than that at the centre frequency. A way to solve this problem is to combine two modes into one single narrow band. However, almost all the two-mode resonance methods reported are for wideband patch antennas because the frequency ratio of two bands is commonly large and hard to decrease. In this article, a detailed mode analysis based on transmission line theory is performed, and a mode shift theory is established for patch antennas. A dual-mode patch antenna with any frequency ratio can be designed. Guided by this theory, a low-profile patch antenna with a size of only $0.23\lambda_0 \times 0.23\lambda_0 \times 0.027\lambda_0$ (λ_0 is the wavelength of the centre frequency in free space) for the Beidou BD3 band (1.258 GHz-1.278 GHz) is designed. The antenna resonates in two modes, and the frequency ratio is only 1.02. The simulated and measured results show that the gain performance of the proposed antenna is almost flat over the operating band (3 dBic-3.1 dBic), which is hard to achieve through any other bandwidth enhancement method.

INDEX TERMS Circular polarization, microstrip antennas, electrically small antenna.

I. INTRODUCTION

In military satellite navigation systems, an adaptive anti-jamming array is generally adopted, and antenna elements for the Beidou BD3 band (1.258 GHz-1.278 GHz) attract much interest. Designing such an array demands miniature antenna elements (or a small ''footprint'' antenna). Due to its compact features, the patch antenna is a good candidate, and many small footprint patch antennas for the BD3 band have been reported.

In addition, to design a conformal anti-jamming array, reducing the height of the antenna element (low profile) is also important. However, the design of a low-profile BD3 patch antenna is quite difficult. As BD3 is a single band (20 MHz), reported BD3 patch antennas commonly resonate in a single mode. For a single mode patch antenna, the smaller the height is, the narrower the bandwidth, which means that if the height of the single mode patch antenna is quite low, the performance of the side frequencies is worse than that of the centre frequency. For a high-performance anti-jamming antenna array, the performance over the whole operating band has to be flat. Increasing the antenna height is the most common method to compensate for the performance discrepancy between the side frequencies and centre frequency. Therefore, the design of a low-profile BD3 patch antenna is quite difficult.

The goal of this article is to design a low-profile patch antenna with an electrical size of only $0.23\lambda_0 \times 0.23\lambda_0 \times 0.027\lambda_0$ (λ_0 is the wavelength of the centre frequency in free space) operating over 1.258 GHz to 1.278 GHz. The small footprint is maintained, and the height of the proposed antenna is only $0.027\lambda_0$ (6.5 mm). The S(1,1) and gain performance of the proposed antenna must be flat, which means that the performance in the centre frequency and side frequencies are the same.

An assumption can be made that if two resonant modes are combined between 1.258 GHz and 1.278 GHz, the height of the antenna can be quite small, and each resonance can be designed narrowly, while the performance over the whole operating band can be flat. The problem mentioned above is solved. However, to reach this goal, the frequency ratio of these two resonant modes must be only 1.02, which is extremely hard.

Many studies have combined two resonant modes to form a wideband, such as adopting an E-shaped patch or annular-ring patch or adding an S-shaped slot [1]–[3]. However, the frequency ratio of the two modes is approximately 1.2-1.3, which is too large. The root idea of these techniques

The associate editor coordinating the review of this manuscript and approving it for publication was Yingsong Li.

cannot be used to achieve the goal in this article because the frequency ratio cannot be smaller. That is why the heights of these antennas are large; hence, each resonance is wideband to form a wider band. If the height of these antennas is decreased, the wideband antenna turns into a dual-band antenna [16].

Using the U-shaped slot [4], dual layer patch [6]–[8], wang-shape [13], Jia-shape patch [14] or stepped-impedance resonator (SIR) technique [5] can achieve a small frequency ratio of approximately 1.1 for the dual mode. However, a small frequency ratio is achieved by increasing the antenna height. This is obvious by comparing references [6]–[8].

Another kind of patch antenna for satellite navigation system is single feed CP patch antenna [17]–[19]. The patch is asymmetry in order to achieve two orthogonal resonant modes with 90° phase difference. In order to achieve 90° phase difference for these two modes, the resonant frequency of these two resonant modes are differential(by the asymmetry structure) by the centre frequency. So, the resonant frequency ratio of these two orthogonal resonant modes is very small with small antenna height. However, there are two serious defects of single feed CP patch antenna: 1)Two close resonant modes are with 90° difference which means only CP radiation can be achieved. If the two modes are with the same phase, this antenna will turn to a single resonant antenna and the bandwidth will decrease. It means that this small frequency ratio method can't be applied to liner polarized patch antenna. 2)Even wide impedance bandwidth can be achieve, the AR bandwidth and RHCP gain bandwidth of this kind of this antenna is very narrow. If an antenna array is implemented, the resonant frequency is very sensitive to other element of the array. Above all, single feed CP patch antenna has defects for high-performance satellite navigation application.

The author have devoted much effort to the mode analysis of patch antennas. In the authors' previous work [9], [10], shorting loads are added to the patch to combine TM_{10}-TM_{50} modes to form a Ultra-wideband operation. However, the frequency ratio of the multi-modes in these antennas is still large. In reference [15], shorting pin load patch antenna is proposed to achieve small frequency ratio. However, the height and the result is still far from the goal of this article.

To achieve the goal of this article, the transmission line mode method is utilized for the patch antenna, and a comprehensive mode shift theory for the patch antenna is established in Section II. Theoretically, the different modes of the patch antenna can be shifted to random frequency points. In Section III, guided by this theory, we design a patch antenna with TM_{10} mode and TM_{30} mode, and the frequency ratio of these two modes is only 1.02. In Section IV of this article, a feed network is designed to achieve CP radiation. By adding this feeding network, we propose a circularly polarized BD3 (1.258 GHz-1.278 GHz) patch antenna with dimensions of only 55 mm×55 mm×6.5 mm ($0.23\lambda_0 \times 0.23\lambda_0 \times 0.027\lambda_0$), which means that the goal of this study is achieved. In Section V, the simulated and measured results are shown, which proves the performance of the proposed band enhancement method.

TABLE 1. The summarized of wideband technique for patch antenna.

reference	technique	height	frequency ratio	bandwidth	Gain (dBi)
[1]	E-shape patch	$0.07\lambda_0$	1.45	26.9% 7.1%	7.1 7.4
[2]	S-shape slot	$0.086\lambda_0$	1.28	16% 12.5	5
[3]	annular-ring	0.01	1.21	5.8% 6%	1.35 3.5
[4]	U-slot patch	$0.085\lambda_0$	1.06	9%	8
[5]	SIR	$0.15\lambda_0$	1.07	10%	7.4
[6]	dual layer patch1	$0.06\lambda_0$	1.2	21%	7
[7]	dual layer patch2	$0.09\lambda_0$	1.1	37%	4
[8]	dual layer patch2	$0.11\lambda_0$	1.05	2.99% 2.72%	4.5
[13]	Wang-shape patch	$0.5\lambda_0$	1.09	9%	12
[14]	Jia-shape patch	$0.1\lambda_0$	1.05	8% 6%	7.3 6.3
[15]	Shorting pin	$0.08\lambda_0$	1.12	18%	8.5
[16]	dual layer patch 4	$0.019\lambda_0$	1.28	2% 1%	4 6
[9]	Coupled shorting load	$0.05\lambda_0$	1.2	32%	4
	This work	$0.027\lambda_0$	1.02	1.7%	3

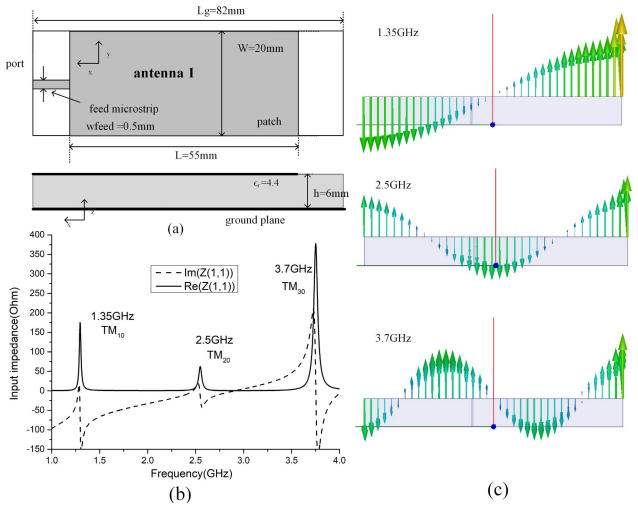

FIGURE 1. (a) The structure of antenna 1 (b) The Z(1,1) of antenna 1 (c) The E-field distribution at the three resonances of antenna 1.

II. THE MODE SHIFT THEORY FOR PATCH ANTENNA

A. THE TRANSMISSION LINE MODE OF THE PATCH ANTENNA

First, a prototype patch antenna (marked as antenna 1) is designed as shown in Fig. 1(a). The dimensions are 55 mm (length)×20 mm (width)×6 mm (height). Rogers TMM4 ($\varepsilon = 2.65\varepsilon_r = 4.4$ and loss tangent=0.002) is used as the substrate, and the patch is fed by the microstrip line to the patch. The simulated Z(1,1) is shown in Fig. 1(b). The FEM

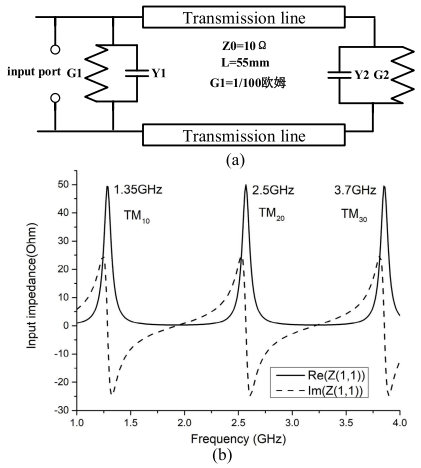

FIGURE 2. (a) Transmission line mode of antenna 1 (b) Z(1,1) of the transmission line mode.

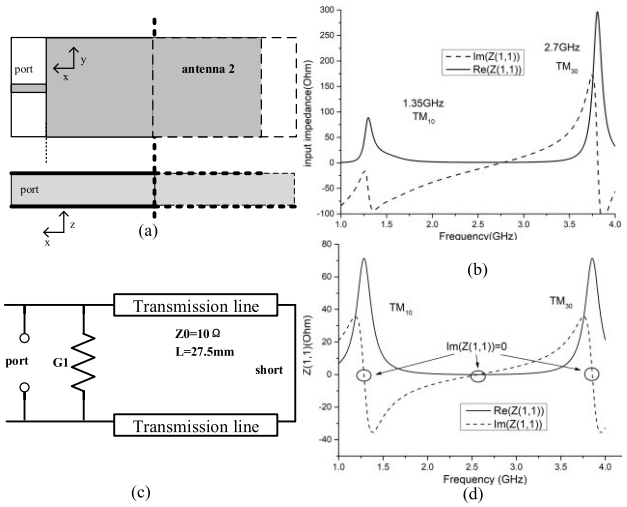

FIGURE 3. (a) The structure of antenna 2 (b) The Z(1,1) of antenna 2 (c) The simplified transmission line mode (d) The Z(1,1) of the transmission line mode.

method in the software Ansys HFSS is used as simulation software in this article.

The patch antenna can be regarded as a resonance cavity surrounded by magnetic boundaries. The resonance mode is TM_{nm} mode. It can be seen from the input impedance in Fig. 1(b) that antenna 1 resonates at 1.35 GHz, 2.5 GHz and 3.7 GHz. The patch is rectangular instead of square to reserve the TM_{n0} mode and restrain the $TM_{nm}(m\neq0)$ mode, which means that only TM_{n0} modes exist. Based on the E-field distribution at these three resonances in Fig. 1(c), these three resonances correspond to the TM_{10}, TM_{20} and TM_{30} modes. Higher modes also exist but are not shown here.

The goal of this article is to randomly shift the resonance frequency. Therefore, a mode shift theory is needed to guide the design. In this article, the derivative of the input impedance of the transmission line mode of the shorting load patch antenna is taken to establish a comprehensive mode shift theory for the patch antenna. The design goal of this article (low-profile BD3 antenna) is an application example of this theory showing that this theory has important guiding significance for the design of patch antennas with exceptional requirements.

The transmission line method is a conventional method for analysing patch antennas. The transmission line mode of antenna 1 is shown in Fig. 2(a). Because the antenna is rectangular and the E-field only changes in one dimension, a part of a one-dimensional transmission line can be used to represent antenna 1. In addition, this model consists of two parallel impedances Y1=G1+jB1 and Y2=G2+jB2 (shown in Fig. 2). G1and G2 are the conductance due to the radiation of the slots, dielectric loss and surface wave loss. Y1 and Y2 are equivalent to an extension of the transmission line. They are capacitive. The calculation of Z_0 and β is shown in Fig. 2(a). The calculation of Y1 and Y2 are present in reference [11] which are not shown in my paper due to the length limit. The Z(1,1) of the transmission line mode is shown in Fig. 2(b). Compared with the Z(1,1) of antenna 1, the position of three resonances represent the three modes (TM_{10}, TM_{20}, and TM_{30} modes) of the transmission line mode are the same with antenna 1. Transmission line mode is a qualitatively design method of patch antenna which means the amplitude of input impedance is not match well with actual antenna. However, the position of the resonant mode matches well and it doesn't affect the research procedure in this article.

The transmission line mode in Fig. 2(a) is complicated and needs to be simplified. Because the transmission line mode is symmetrical, a PEC wall is added in the middle of the antenna, as shown in Fig. 3(a). This antenna is marked antenna 2. Based on the mirror theory, the transmission line mode can be simplified as shown in Fig. 3(c). The only difference is that the even mode is eliminated and only TM_{10} and TM_{30} modes exist. This is because the PEC wall minimizes the E-field in the middle of the antenna (as shown in Fig. 1(c)), and the TM_{20} mode can't exist. Studying the mode shifts of TM_{10} and TM_{30} is sufficient for us to establish the theory. The Z(1,1) of antenna 2 is shown in Fig, 3(b) and its transmission line mode is shown in Fig. 3(d). The position of resonant mode matches well.

B. THE EFFECT OF DIRCTED SHORTING LOAD FOR PATCH ANTENNA

The realization of the mode shift is structurally based on the shorting load at different positions on the patch. There are mainly two kinds of shorting loads. The coupled shorting load is where the shorting pins are coupled to the patch, as shown in Fig. 4(a) and this antenna is marked as antenna 2-1; the directed shorting load is where the shorting pins are directly connected to the patch and this antenna is marked as antenna 2-2, as shown in Fig. 4(b). For the transmission line mode, the coupled shorting load can be regarded as an inductance in series with a capacitance in parallel with the transmission line, and the directed shorting load can be regarded as an inductance in parallel with the transmission line, as shown in Fig. 4.

The parameters of lumped elements in Fig.4 are roughly calculated based on the size of the shorting load(the length

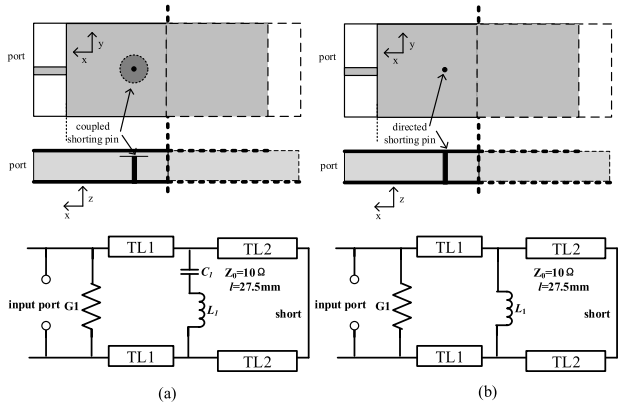

FIGURE 4. (a) The structure and transmission line mode of the coupled shorting load antenna(antenna2-1). (b) The structure and transmission line mode of the directed shorting load antenna(antenna2-1).

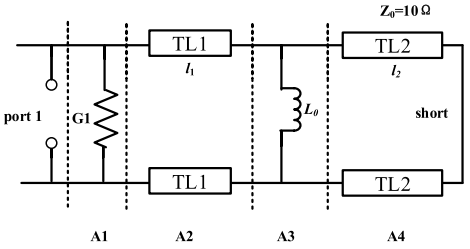

FIGURE 5. Transmission line mode of the directed shorting load patch antenna.

and radius of directed shorting load and the gap between the patch and the coupled load). After that, tune tool of the circuit simulation software is used to tune the parameters of lumped elements to make the impedance of transmission line mode match the rational result. Even the parameters of these lumped element is not accurate due to the element with distributed parameters can't be equal to lumped elements. The goal of utilizing transmission line mode is to study of the position of the shorting load qualitatively. The parameters of the lumped elements in Fig. 4 (L_1 and C_1) have little qualitative influence on the conclusion of the research.

When loading the shorting load at different positions of the patch, the effect on the different modes is different, and that position is the research object.

In this section, we begin with the directed shorting load antenna 2-2 in Fig. 4(b). First, the goal of this section is to obtain the input impedance of the directed shorting load patch antenna (Z(1,1) shown in Fig. 4 and 5). The procedure is as follows:

1) First, separate the transmission line mode shown in Fig. 5 into four parts;

2) Second, obtain the matrix A of these four parts (A1-A4);

3)Third, use matrix cascading to obtain A=A1∗A2∗A3∗A4;

4) Last, use the A-Z matrix transformation to obtain Z(1,1);

The matrix A of the four parts is:

$$A_1 = \begin{bmatrix} 1 & 0 \\ g_1 & 1 \end{bmatrix} \tag{1}$$

$$A_2 = \begin{bmatrix} \cos(\beta * l_1) & jZ_0 \sin(\beta * l_1) \\ jY_0 \sin(\beta * l_1) & \cos(\beta * l_1) \end{bmatrix} \tag{2}$$

$$A_3 = \begin{bmatrix} 1 & 0 \\ 1/(j\omega L_0) & 1 \end{bmatrix} \tag{3}$$

$$A_4 = \begin{bmatrix} 1 & 0 \\ 1/(jZ_0 \tan(\beta * l_2)) & 1 \end{bmatrix} \tag{4}$$

$$A = A_1 * A_2 * A_3 * A_4 \tag{5}$$

$$Z(1,1) = A(1,1)/A(2,1) \tag{6}$$

$$l_1 + l_2 = 27.5\text{mm} \times \sqrt{\varepsilon_r}, \quad Z_0 = 8\Omega, \quad L_0 = 0.3nH, \; g_1 = 1/50, \; \varepsilon_r = 4.5 \tag{7}$$

By solving equations (1)-(5), we can obtain:

$$\begin{aligned} A &= \begin{bmatrix} A(1,1) & A(1,2) \\ A(2,1) & A(2,2) \end{bmatrix} \\ A(1,1) &= \cos(\beta l_1) + \frac{Z_0 \sin(\beta l_1)}{\omega L_0} + \cot(\beta l_2)\sin(\beta l_1) \\ A(1,2) &= jZ_0 \sin(\beta l_1) \\ A(2,1) &= g_1 \cos(\beta l_2) + \frac{j\sin(\beta l_1)}{Z_0} \\ &\quad - \frac{j(\cos(\beta l_1) + g_1 jZ_0 \sin(\beta l_1))}{L_0 \omega} \\ &\quad + \frac{j\cot(\beta l_2)(\cos(\beta l_1) + g_1 jZ_0 \sin(\beta l_1))}{Z_0} \\ A(2,2) &= \cos(\beta l_1) + g_1 jZ_0 \sin(\beta l_1) \end{aligned} \tag{8}$$

Substituting (8) into (6);

$$\begin{aligned} Z(1,1) &= \frac{A(1,1)}{A(2,1)} = \frac{A}{B + jC} \\ A &= \cos(\beta l_1) + \frac{Z_0 \sin(\beta l_1)}{\omega L_0} + \cot(\beta l_2)\sin(\beta l_1) \\ B &= g_1 \cos(\beta l_2) + \frac{g_1 jZ_0 \sin(\beta l_1)}{L_0 \omega} \\ &\quad - \frac{\cot(\beta l_2) g_1 Z_0 \sin(\beta l_1)}{Z_0} \\ C &= \frac{\sin(\beta l_1)}{Z_0} - \frac{\cos(\beta l_1)}{L_0 \omega} + \frac{\cot(\beta l_2)\cos(\beta l_1)}{Z_0} \end{aligned} \tag{9}$$

The input impedance of the transmission line mode without any loading is shown in Fig. 3(d). It can be seen that the antenna resonates when the imaginary part of the impedance equals zero. Relating with Fig. 3(d), it can be seen that, the first resonant point and the 3rd resonant point which is parallel resonant represents TM_{10} and TM_{30} mode while the 2nd resonant point is neglect which is a serial resonant point. which means:

$$\begin{aligned} Im(Z(1,1)) &= -\frac{AC}{B^2 + C^2} = 0 \\ AC &= 0 \\ &\left[\cos(\beta l_1) + \frac{Z_0 \sin(\beta l_1)}{\omega L_0} + \cot(\beta l_2)\sin(\beta l_1)\right] \\ &\times \left[\frac{\sin(\beta l_1)}{Z_0} - \frac{\cos(\beta l_1)}{L_0 \omega} + \frac{\cot(\beta l_2)\cos(\beta l_1)}{Z_0}\right] = 0 \end{aligned} \tag{10}$$

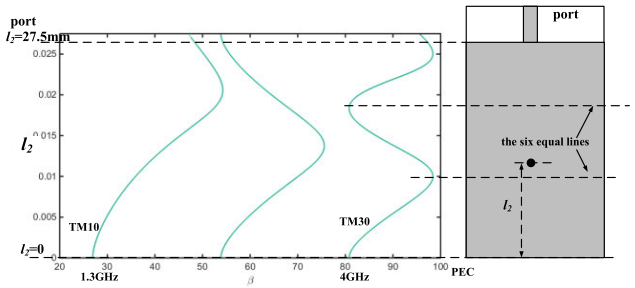

FIGURE 6. The relationship between l_2 and β for directed shorting load.

Substituting (7) and (9) into (10), we can obtain a relationship between l_2 and β, where Im(Z(1,1)=0) and β is the propagation constant of the transmission line mode. MATLAB is used to depict (10), as shown in Fig. 6.

The result in Fig. 6 can be obviously connected with the E-field distribution in Fig. 1(c). First, if the shorting probes are loaded in the middle of the patch (the minimum E-field of TM_{10} mode, $l_2 = 0$ mm), the resonant frequency of TM_{10} is the same as that of antenna 2 and is the lowest. When the shorting probes are moved to the edge of the patch (increasing l_2), the resonant frequency of the TM_{10} mode increases (moving the minimum E-field of the TM_{10} mode towards the maximum E-field of the TM_{10} mode).

Second, if the shorting probes are loaded in the middle of the patch (the minimum E-field of TM_{30} mode, $l_2 = 0$ mm), the resonant frequency of TM_{30} is the same as that of antenna 2 and is the lowest. When the shorting probes are moved to the edge of the patch (increasing l_2), the resonant frequency of the TM_{30} mode first increase (moving the minimum E-field of the TM_{30} mode towards the maximum E-field of the TM_{30} mode, the trisection line) and then decreases (moving the maximum E-field of the TM_{30} mode (the six equal lines) towards another minimum E-field of the TM_{30} mode). When the shorting probes are loaded at the edge of the patch (the maximum E-field of TM_{30} mode, $l_2 = 27.5$ mm), the resonant frequency of TM_{30} is the highest.

The effect of the directed shorting load on the patch antenna can be summarized as follows: The directed shorting load increases the resonance frequencies of different modes of the patch antenna based on the loading position. If the directed shorting load is added to the maximum E-field area of a certain mode, the resonant frequency of this mode increases the most; if the directed shorting load is added to the minimum E-field area of a certain mode, the resonant frequency of this mode remains unchanged.

C. THE EFFECT OF COUPLED SHORTING LOAD FOR PATCH ANTENNA

The study procedure is the same as that for the directed shorting load patch antenna. What is different from the directed shorting load antenna is that the inductance load changes to an inductance in series with a capacitance($L_0 = 0.1nH$, $C_0 = 10pF$), as shown in Fig. 7, which means that the derivation procedure is exactly the same as that for directed shorting

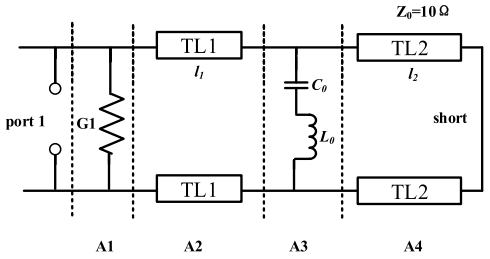

FIGURE 7. Transmission line mode of the coupled shorting load patch antenna.

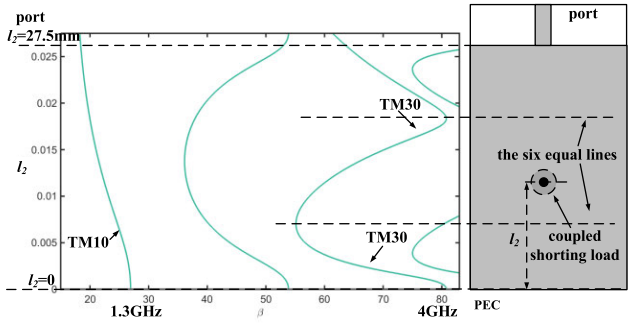

FIGURE 8. The relationship between l_2 and β for coupled shorting load.

load antenna, except the A3 matrix becomes:

$$A_3 = \begin{bmatrix} 1 & 0 \\ \dfrac{1}{j\omega L_0 + \frac{1}{j\omega C_0}} & 1 \end{bmatrix} \tag{11}$$

Therefore, the derivation procedure is omitted, and the result is shown in Fig. 8. The effect of the coupled shorting load and on the resonance frequency obviously mirrors that of the directed shorting load.

First, if the shorting probes are loaded at the centre of the patch (the minimum E-field of TM_{10} mode, $l_2 = 0$ mm), the resonant frequency of TM_{10} is the same as that of antenna 2 and is the highest. When the shorting probes are moved to the edge of the patch (increasing l_2), the resonant frequency of the TM_{10} mode decreases (moving the minimum E-field of the TM_{10} mode towards the maximum E-field of the TM_{10} mode).

Second, if the shorting probes are loaded at the centre of the patch (the minimum E-field of TM_{30} mode, $l_2 = 0$ mm), the resonant frequency of TM_{30} is the same as that antenna 2 and is the highest. When the shorting probes are moved to the edge of the patch (increasing l_2), the resonant frequency of the TM_{30} mode first decreases (moving the minimum E-field of the TM_{30} mode towards the maximum E-field of the TM_{30} mode, the trisection line) and then increases (moving the maximum E-field of the TM_{30} mode (the trisection line) towards another minimum E-field of the TM_{30} mode). If the shorting probes are loaded at the edge of the patch (the maximum E-field of TM_{30} mode, $l_2 = 27.5$ mm), the resonant frequency of TM_{30} is the lowest.

Therefore, the effect of the coupled shorting load on the patch antenna can be summarized as follows: The coupled

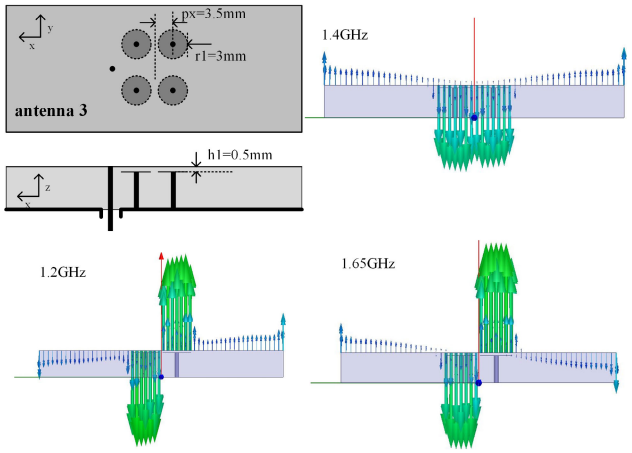

FIGURE 9. The structure of antenna 3 and the E-field distribution at the three resonances.

shorting load decreases the resonance frequency of different modes of the patch antenna based on the loading position. If the coupled shorting load is added to the maximum E-field area of a certain mode, the resonant frequency of this mode decreases the most; if the coupled shorting load is added to the minimum E-field area of a certain mode, the resonant frequency of this mode remains unchanged.

Combined with the conclusion in Section II B and C of antenna 2-1 and 2-2, the mode shift theory is established in this article. If a certain mode is selected and the E-field distribution is obtained, through loading with directed or coupled shorting load at a certain position, the resonant frequency can be moved randomly.

III. THE DESIGN OF LINER POLARIZED LOW PROFILE PATCH ANTENNA

A. THE COUPLED SHORTING LOAD PATCH ANTENNA

In this section, the first part of the mode shift theory is used to move the resonance of the TM_{30} mode closer to that of the TM_{10} mode. As shown in Fig. 8, if the coupled shorting load is added to the centre area of the patch, the resonant frequency of the TM_{30} mode decreases faster than that of the TM_{10} mode, and the distance between the TM_{10} and TM_{30} modes is the shortest. Therefore, four coupled shorting probes are added to antenna 1, as shown in Fig. 9, and this antenna is marked antenna 3. A probe feed configuration is adopted to achieve impedance matching. The positions of these coupled shorting probes are in the centre area of the patch (px=3.5 mm). The S(1,1) comparison between antenna 1 and antenna 3 is shown in Fig. 10. The antenna resonances at 1.2 GHz, 1.45 GHz and 1.6 GHz and the E-field distribution at these three frequencies are shown in Fig. 9. It is obvious that these three resonances correspond to the TM_{10}, TM_{20} and TM_{30} modes.

The parameter study (position of shorting probe in the direction of the E-field changes) of antenna 3 is shown in Fig. 11. The influence of the position of the shorting probe on these three modes is in agreement with Fig. 8.

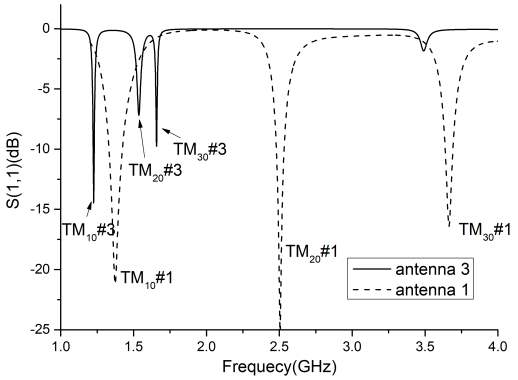

FIGURE 10. The S(1,1) of antenna 1 and antenna 3.

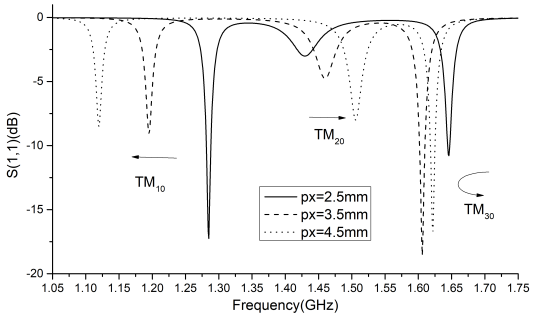

FIGURE 11. The effect of the position of the shorting load of antenna 3.

B. THE COMBINATION OF THE TM10 AND TM30 MODES OF THE PATCH ANTENNA

Antenna 3 is far from the goal of this article: the combination of two modes is not realized. There are two problems that need to be solved.

1) For a patch antenna for a satellite navigation system, a unidirectional radiation pattern is necessary. An even mode (TM_{n0}, n=2,4…) leads to an omnidirectional radiation pattern, which must be suppressed. People use differential feed configurations to eliminate even modes [10]. In this configuration, two feed points are symmetrical in the patch with a phase difference of 180°. To obtain CP radiation and a differential feed at the same time, a four-feed feed network with the same amplitude and phases of 0°, 90°, 180°, and 270° is needed. However, in this article, for a small footprint antenna, the transverse dimension is not sufficient for a four-feed network. The two-feed configuration is the only feasible feed method to achieve CP radiation. Hence, differential feed technology is impractical in this article. The even mode (TM_{20}) cannot be eliminated.

The only way to solve this problem is to combine two odd modes of the patch antenna (TM_{10} and TM_{30} mode). However, as shown in Fig. 11, for antenna 3, the resonant frequency TM_{20} mode lies between TM_{10} and TM_{30} modes. Therefore, we have to shift the TM_{20} mode somewhere else other than between the TM_{10} and TM_{30} modes.

2) As shown in Fig. 8 and Fig. 11, for antenna 3, the frequency ratio of TM_{10}-TM_{30} modes is still large, which is far from the goal of this article (1.02).

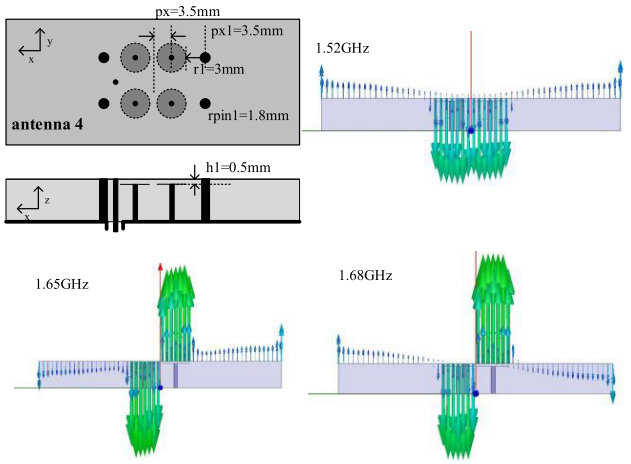

FIGURE 12. The structure of antenna 4 and the E-field distributions at the three resonances.

As shown in Figs. 6 and 8 in Section II, these two problems cannot be solved by separately adopting the coupled shorting or directed shorting load. Therefore, in this section, a new design procedure is proposed: these two kinds of shorting probes must be combined.

First, the minimum E-field area of the TM_{20} and TM_{30} modes of antenna 3 are found. As shown in Fig. 9, the area is outside and near the coupled shorting loads.

Second two pairs of directed shorting loads are placed in the specific position of procedure 2.

Last, the position and size of the shorting loads are optimized.

Let us explain why these two steps can achieve the goal. In antenna 3, the coupled probes are loaded in the centre to decrease the resonant frequency of TM_{20} and TM_{30} mode to make them close to TM_{10} mode. The goal in the first step is to increase the resonant frequency of the TM_{10} mode higher than that of the TM_{20} mode and lower than that of the TM_{30} mode, which means that the TM_{10} and TM_{30} modes are adjacent and can be combined. The specific position in this step is the minimum E-field position of the TM_{30} of the antenna 3. In addition to the TM_{30} mode, this position is also the minimum E-field position of TM_{20} but is not the minimum E-field position of the TM_{10} mode. Therefore, this pair of directed shorting probes in this specific position increase the resonance frequency of the TM_{10} mode while the resonant frequencies of the TM_{20} and TM_{30} modes remain unchanged. In this way, the resonant frequency of the TM_{20} mode is lower than that of the TM_{10} mode, and the goal is achieved. This new antenna is marked antenna 4.

The structure of antenna 4 is shown in Fig. 12. The S(1,1) of antenna 4 is shown in Fig. 13. The three resonant frequencies are 1.52 GHz 1.65 GHz and 1.68 GHz. The E-field distributions of these three frequencies are shown in Fig. 12. First, the resonance at the lowest frequency is the TM_{20} mode, which is below the TM_{10} and TM_{30} modes. Second, the frequency ratio of the TM_{10} and TM_{30} modes significantly decreases to 1.02 from 2. The design goal of this section is achieved.

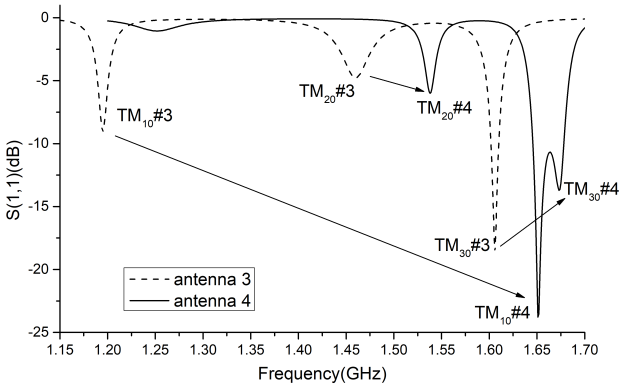

FIGURE 13. The S(1,1) of antenna 3 and antenna 4.

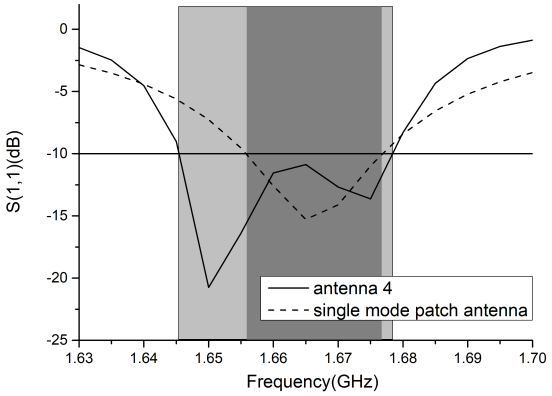

FIGURE 14. The S(1,1) of antenna 1 and antenna 4.

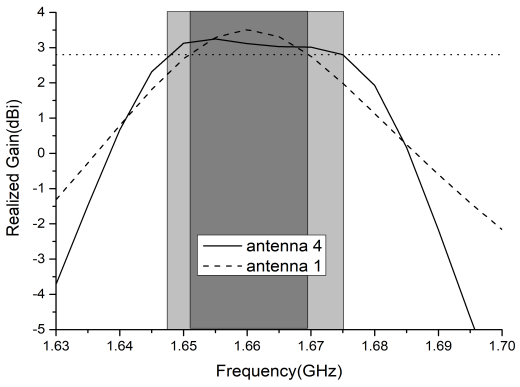

FIGURE 15. The realized gain comparison of antenna 1 and antenna 4.

C. THE COMPARISON OF ANTENNA 1 AND ANTENNA 4

To prove the bandwidth enhancement effect of this method, the resonant frequency of antenna 1 is slightly shifted to 1.65 GHz, and antenna 4 and antenna 1 are compared in Fig. 14 and 15. It can be seen that by combining two modes, we significantly increase the impedance and gain bandwidth compared with those of the single mode patch antenna.

IV. THE DESIGN OF CIRCULARLY POLARIZED LOW PROFILE PATCH ANTENNA FOR BD3 BAND

A. THE DESIGN OF FEED NETWORK

To achieve CP radiation, a two-feed feed network (with same amplitude and phase of 0°, 90° is designed.

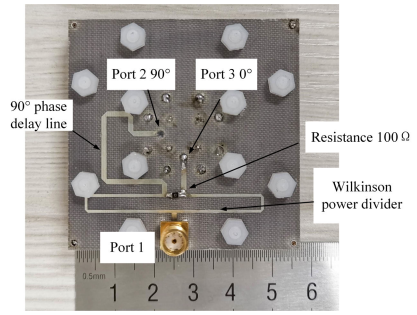

FIGURE 16. The fabricated photos of feed network.

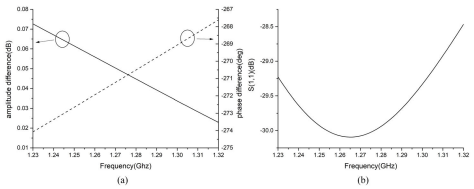

FIGURE 17. The (a) S(1,1) (b)magnitudes and phase difference.

The feed network (microstrip line) is shown in Fig. 16. It comprises a Wilkinson power divider in cascade with a 90° phase shifter.

The performance of the feed network is shown in Fig. 17. The S(1,1), magnitude and phase unbalance is quite desirable over the whole operating band.

B. THE CONFIGURATION OF CP LOW PROFILE PATCH ANTENNA

Firstly, in order to achieve CP radiation, two orthogonal liner polarized is needed. So, antenna 4 is redesigned as shown in Fig. 18. Two liner polarized antenna (antenna 4) is orthogonal put and excited by the two outputs of the feed network respectively with same amplitude and phase of 0°, 90°. Square patch is adopted and the antenna structure is center symmetry.

Second, antenna 4 resonates at 1.67 GHz. To achieve TM_{10} and TM_{30} resonances at arbitrary bands, four coupled shorting loads are added at four corners of the patch. As shown in Fig. 6, the edge of the patch is the maximum E-field area of the TM_{10}-TM_{30} modes. Therefore, if the coupled shorting loads are added to the edge of the patch, the resonant frequencies of these three modes are decreased at the same speed. Thus, four coupled shorting loads are added to the edge of the patch to make the antenna resonate at 1.258 GHz-1.278 GHz.

This antenna is the final design of this article, marked as antenna 5. TP-1 (relative dielectric constant $\varepsilon = 2.65\varepsilon_r = 4.4$ and loss tangent=0.001) is used as the substrate. The feed network in the form of a microstrip line is on the back side of the bottom layer. Two outputs of the feed network are directly connected to the patch in the top layer. Four of the coupled shorting loads are coupled to the patch in the centre area of the patch, and the other four are added to the edge of the patch. Eight directed shorting loads are shorted to the ground plane from the patch. F4B with thickness=0.5 mm

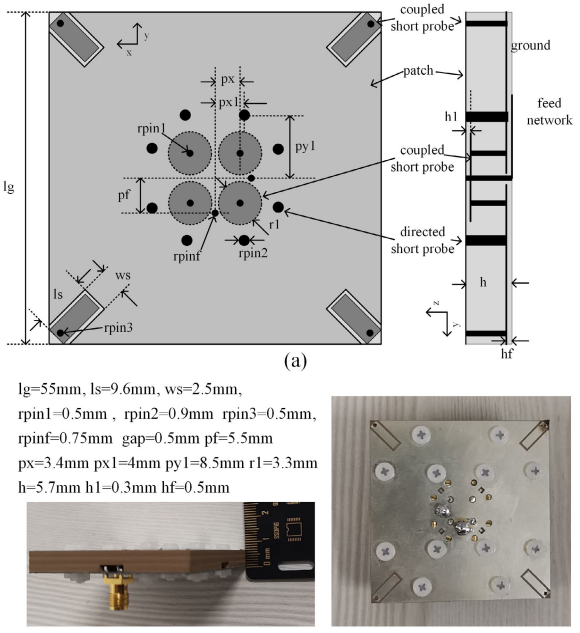

FIGURE 18. (a)The structure of final CP patch antenna (b)The fabricated photo.

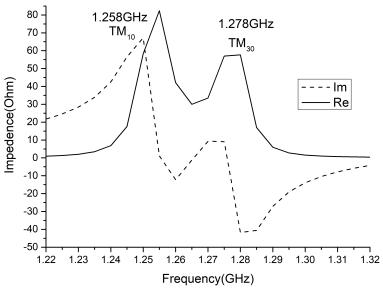

FIGURE 19. The input impedance of antenna 5.

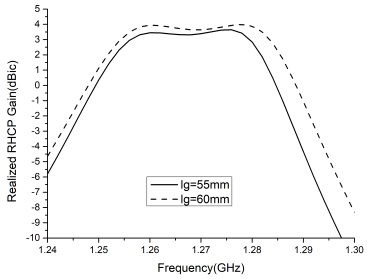

FIGURE 20. The gain comparison different size of ground plane of antenna 5.

(relative dielectric constant$\varepsilon = 2.65\varepsilon_r = 2.65$ and loss tangent=0.002) is used as the top layer and the substrate of the feed network. The height of the antenna is 6 mm, and the height of the feed network is 0.5 mm, which means that the final height of the CP antenna is 6.5 mm.

The input impedance of antenna 5 (without a feed network) is shown in Fig. 19. The two resonances correspond to the TM_{10} and TM_{30} modes and are at 1.258 GHz and 1.278 GHz.

The size of the ground mainly affect the gain performance of patch antenna(larger ground size means higher gain).

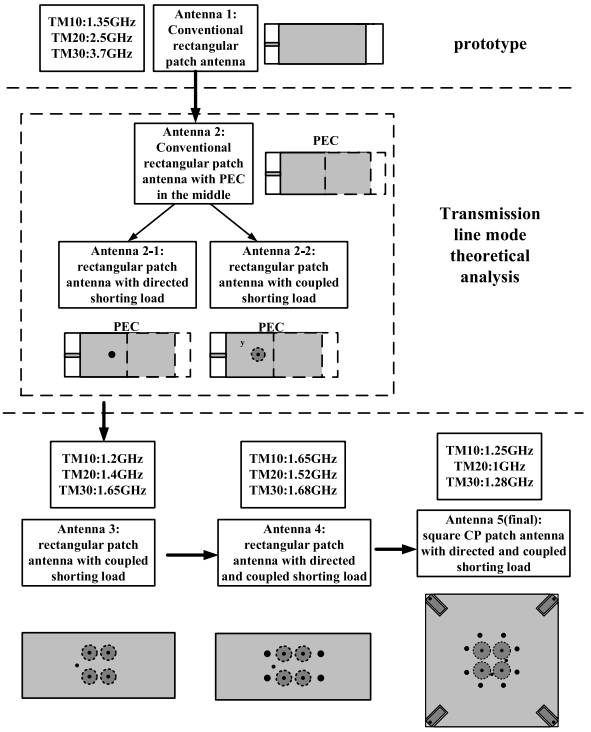

FIGURE 21. The design flowchart.

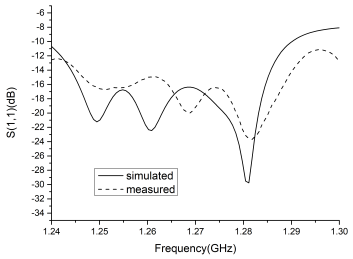

FIGURE 22. Simulated and measured S(1,1).

It will affect the position of the resonant frequency slightly while not the design method. Another antenna 5 with ground plane size lg=60mm is designed only by slightly changing the parameters (lg=60mm, px=3.5mm, py1=8.7mm, r1=3.32mm, ls=7.6mm). The length of the shorting load in the corner of the patch is reduced from 9.6mm to 7.6mm in order to compensate the increase of the patch size. The position of the coupled and directed shorting load in the center of the patch is slight increased due to the size of patch is increased. Other parameters are almost the same. The gain comparison is shown in Fig. 20 and the gain performance of antenna 5 with 60mm ground plane is higher than that of 55mm while the gain bandwidth is almost the same.

The whole design procedure from the initial assumption to the final design is shown in Fig. 21 as a flowchart.

V. THE RESULTS AND DISCUSSION

The simulated and measured and S(1,1) of antenna 5 with feed network is shown in Fig. 22, which is below −15 dB over 1.258GHz-1.278GHz. The radiation performance is measured in Microwave anechoic chamber. The simulated and

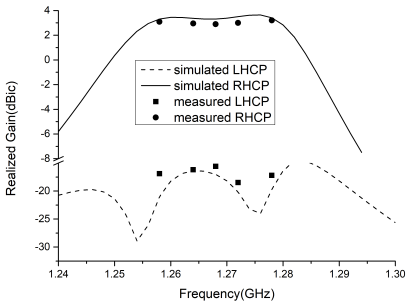

FIGURE 23. Simulated and measured boresight RHCP and LHCP gain verse frequency.

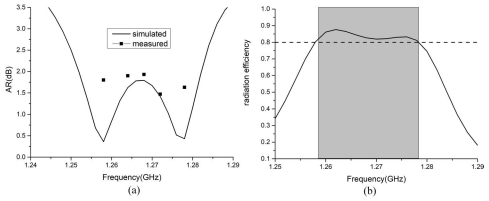

FIGURE 24. Simulated and measured boresight (a)AR and (b)radiation efficiency verse frequency.

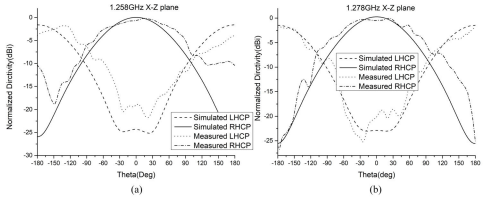

FIGURE 25. Simulated and measured normalization directivity pattern in (a)1.258GHz (b)1.278GHz.

measured RHCP gain and LHCP gain verse frequency is shown in Fig. 23. The realized gain is flat over the whole operating band(3dBic-3.1dBic). The simulated and measured AR versus frequency is shown in Fig. 24(a) which is below 0.2 and the radiation efficiency is show in Fig. 24(b) which is above 0.8 over the operating band. The radiation pattern in two edge frequencies is measured and compared with simulated result as shown in Fig. 25, with AR pattern in Fig. 26. It can be seen that the gain performance in two edge frequencies is almost the same as center frequency. There is some mismatch of the simulated and measured result due to the error of the fabrication. The size of the antenna is quite small and the fabrication error is hard to avoid.

In order to show the performance advantages over the exist designs, the final design is compared with miniature patch antennas with bandwidth enhancement proposed in [12], [18], [19] as shown in Table 2. Compared with single mode patch antenna with bandwidth enhancement method [12], the height of proposed antenna is significant reduced while the gain discrepancy is reduced. Compared with single feed patch antenna with same height [18], the gain discrepancy is significant reduced. Compared with single feed patch antenna with same bandwidth [19], the height is significant reduced. The proposed small frequency ratio dual mode patch shows performance advantages over all the single mode

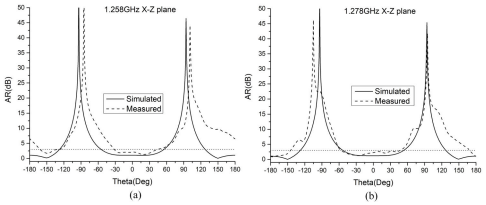

FIGURE 26. Simulated and measured AR pattern in (a)1.258GHz (b)1.278GHz.

TABLE 2. Comparison between antenna 5 and other antennas.

reference	size	height	gain discrepancy	Gain bandwidth	AR bandwidth
[12] two feed single mode	$0.15\lambda_0$	$0.06\lambda_0$	0.3dBic(2-2.3dBic)	1.7%	3%
[18] single feed	$0.31\lambda_0$	$0.026\lambda_0$	0.65dBic	1.7%	1.7%
[19] single feed	0.16	$0.08\lambda_0$	0.3dBic	1.6%	1.6%
This paper	$0.23\lambda_0$	$0.027\lambda_0$	flat, 0.1dBic(3-3.1dBic)	1.7%	3%

patch antennas and it solves the conflict between height and frequency ratio.

VI. CONCLUSION

In this article, to solve the bandwidth problem of a low-profile patch antenna, the effects of directed shorting load and coupled shorting load on the resonant frequencies of different patch antenna resonance modes are studied. A mode shift theory is summarized. By utilizing this theory, we can randomly shift the resonance modes of the patch antenna, and the frequency ratio of the dual band patch antenna can be extraordinarily small. Two bands that are narrow and close to each other can be combined to enhance the bandwidth of the patch antenna. A low-profile patch antenna with a size of only $0.23\lambda_0 \times 0.23\lambda_0 \times 0.027\lambda_0$ (λ_0 is the wavelength of the centre frequency in free space) for the Beidou BD3 band (1258 MHz-1278 MHz) is designed. The antenna resonates in two modes, and the frequency ratio is only 1.02. The simulated and measured results show that the gain performance of the proposed antenna is almost flat over the operating band (3 dBic-3.1 dBic), which is hard to achieve by any other bandwidth enhancement method.

This new proposed technique solves the problem of combining more modes of patch antennas and provides new design guidance for low-profile wideband patch antennas.

REFERENCES

[1] S. Liu, W. Wu, and D.-G. Fang, "Single-feed dual-layer dual-band E-shaped and U-slot patch antenna for wireless communication application," *IEEE Antennas Wireless Propag. Lett.*, vol. 15, pp. 468–471, 2016.
[2] Nasimuddin, Z. N. Chen, and X. Qing, "Dual-band circularly polarized S-shaped slotted patch antenna with a small frequency-ratio," *IEEE Trans. Antennas Propag.*, vol. 58, no. 6, pp. 2112–2115, Jun. 2010.
[3] X. L. Bao and M. J. Ammann, "Dual-frequency circularly-polarized patch antenna with compact size and small frequency ratio," *IEEE Trans. Antennas Propag.*, vol. 55, no. 7, pp. 2104–2107, Jul. 2007.
[4] K.-F. Tong and T.-P. Wong, "Circularly polarized U-slot antenna," *IEEE Trans. Antennas Propag.*, vol. 55, no. 8, pp. 2382–2385, Aug. 2007.
[5] N.-W. Liu, L. Zhu, W.-W. Choi, and J.-D. Zhang, "A novel differential-fed patch antenna on stepped-impedance resonator with enhanced bandwidth under dual-resonance," *IEEE Trans. Antennas Propag.*, vol. 64, no. 11, pp. 4618–4625, Nov. 2016.
[6] Nasimuddin, K. P. Esselle, and A. K. Verma, "Wideband circularly polarized stacked microstrip antennas," *IEEE Antennas Wireless Propag. Lett.*, vol. 55, pp. 84–99, 2014.
[7] D. Li, P. Guo, Q. Dai, and Y. Fu, "Broadband capacitively coupled stacked patch antenna for GNSS applications," *IEEE Antennas Wireless Propag. Lett.*, vol. 11, pp. 701–704, 2012.
[8] Z. Wang, R. She, J. Han, S. Fang, and Y. Liu, "Dual-band dual-sense circularly polarized stacked patch antenna with a small frequency ratio for UHF RFID reader applications," *IEEE Access*, vol. 5, pp. 15260–15270, 2017.
[9] C. Sun, Z. Wu, and B. Bai, "A novel compact wideband patch antenna for GNSS application," *IEEE Trans. Antennas Propag.*, vol. 65, no. 12, pp. 7334–7339, Dec. 2017.
[10] C. Sun, "A design of compact ultrawideband circularly polarized microstrip patch antenna," *IEEE Trans. Antennas Propag.*, vol. 67, no. 9, pp. 6170–6175, Sep. 2019.
[11] H. Pues and A. V. D. Capelle, "Accurate transmission-line model for the rectangular microstrip antenna," *IEE Proc. H, Microw., Opt. Antennas*, vol. 131, no. 6, pp. 334–340, Dec. 1984.
[12] C. Sun, H. Zheng, L. Zhang, and Y. Liu, "Analysis and design of a novel coupled shorting strip for compact patch antenna with bandwidth enhancement," *IEEE Antennas Wireless Propag. Lett.*, vol. 13, pp. 1477–1481, 2014.
[13] S. Sharma and S. Sharma, "Design of high gain wang shape microstrip patch antenna for wireless system," in *Proc. 3rd Int. Conf. Comput., Commun. Netw. Technol. (ICCCNT)*, Jul. 2012, pp. 1–3.
[14] K. L. Chung, X. Yan, Y. Li, and Y. Li, "A Jia-shaped artistic patch antenna for dual-band circular polarization," *AEU-Int. J. Electron. Commun.*, vol. 120, Jun. 2020, Art. no. 153207.
[15] J. Wu, X. Ren, Z. Wang, and Y. Yin, "Broadband circularly polarized antenna with L-shaped strip feeding and shorting-pin loading," *IEEE Antennas Wireless Propag. Lett.*, vol. 13, pp. 1733–1736, 2014.
[16] Nasimuddin, M. F. Karim, and A. Alphones, "A low-profile dual-band circularly polarized GPS antenna," in *Proc. Asia–Pacific Microw. Conf. (APMC)*, New Delhi, India, Dec. 2016, pp. 1–4.
[17] Nasimuddin, Y. S. Anjani, and A. Alphones, "A wide-beam circularly polarized asymmetric-microstrip antenna," *IEEE Trans. Antennas Propag.*, vol. 63, no. 8, pp. 3764–3768, Aug. 2015.
[18] Nasimuddin, X. Qing, and Z. N. Chen, "A compact circularly polarized slotted patch antenna for GNSS applications," *IEEE Trans. Antennas Propag.*, vol. 62, no. 12, pp. 6506–6509, Dec. 2014.
[19] S. Chao, "Analysis and design of a compact circularly polarized microstrip antenna with cross-shape shorting strips," in *Proc. IEEE Int. Conf. Commun. Problem-Solving (ICCP)*, Guilin, China, Oct. 2015, pp. 408–411.

CHAO SUN received the B.Eng. and Ph.D. degrees in electromagnetics from Xidian University, Xi'an, China, in 2011 and 2016, respectively. He is currently a Lecturer with the School of Aerospace Science and Technology, Xidian University. His research interests include miniaturization of microstrip antenna and wideband microstrip antenna.